



OPEN ACCESS

EDITED BY

Antonella Leone,
Istituto di Scienze delle Produzioni Alimentari,
Italy

REVIEWED BY

Zhangxi Hu,
Guangdong Ocean University, China
Laura Biessy,
Cawthron Institute, New Zealand

*CORRESPONDENCE

Wenlu Lan

✉ dr.lan@139.com

Uwe John

✉ Uwe.John@awi.de

RECEIVED 24 February 2025

ACCEPTED 22 April 2025

PUBLISHED 14 May 2025

CITATION

Xu Y, Wang X, Hörstmann C,
Dzhembekova N, Zhu X, Neuhaus S, Tong M,
Lan W and John U (2025) The first recorded
fish-killing bloom in the Beibu Gulf, China:
caused by dinoflagellate *Karenia selliformis*.
Front. Mar. Sci. 12:1582234.
doi: 10.3389/fmars.2025.1582234

COPYRIGHT

© 2025 Xu, Wang, Hörstmann, Dzhembekova,
Zhu, Neuhaus, Tong, Lan and John. This is an
open-access article distributed under the terms
of the [Creative Commons Attribution License
\(CC BY\)](https://creativecommons.org/licenses/by/4.0/). The use, distribution or reproduction
in other forums is permitted, provided the
original author(s) and the copyright owner(s)
are credited and that the original publication
in this journal is cited, in accordance with
accepted academic practice. No use,
distribution or reproduction is permitted
which does not comply with these terms.

The first recorded fish-killing bloom in the Beibu Gulf, China: caused by dinoflagellate *Karenia selliformis*

Yixiao Xu¹, Xi Wang¹, Cora Hörstmann², Nina Dzhembekova³,
Xueming Zhu⁴, Stefan Neuhaus², Mengmeng Tong⁵,
Wenlu Lan^{6*} and Uwe John^{2*}

¹Key Laboratory of Environment Change and Resources Use in Beibu Gulf, Ministry of Education, Nanning Normal University, Nanning, China, ²Alfred-Wegener-Institute Helmholtz Centre for Polar and Marine Research, Bremerhaven, Germany, ³Institute of Oceanology–Bulgarian Academy of Sciences, Varna, Bulgaria, ⁴Southern Marine Science and Engineering Guangdong Laboratory (Zhuhai), Zhuhai, China, ⁵Ocean College, Zhejiang University, Zhoushan, China, ⁶Beibu Gulf Marine Ecological Environment Field Observation and Research Station of Guangxi, Marine Environmental Monitoring Center of Guangxi, Beihai, China

The Beibu Gulf is located in the northwestern South China Sea. On August 2, 2023, a mass mortality event of cultured *Trachinotus ovatus* occurred in Lianzhou Bay and Tieshan Bay, suspected to be associated with a *Karenia* bloom. To identify the causative organism, investigate possible environmental drivers for bloom development, and determine the cause of fish mortality, *in-situ* bloom samples were collected for community characterization and toxicity analysis. Results showed that during the bloom, seawater quality remained within China's highest classification, Class I, and RDA analyses indicated that protistan communities were primarily influenced by dissolved inorganic nitrogen (DIN) and pH. Based on a combination of microscopic observation, phylogenetic analyses of ITS and D1-D3 rDNA sequences obtained from clone libraries, and 18S rDNA V4 amplicon sequence variant (ASV) analysis, all approaches confirmed *Karenia selliformis* as the bloom-causing organism. Weak westward sea surface winds before and during the period facilitated the accumulation and probably the bloom formation of *K. selliformis* in Lianzhou and Tieshan coastal waters. A rabbit erythrocyte lysis assay detected hemolytic toxicity of 45.2–48.3% in tests with 5×10^7 rabbit erythrocyte cells exposed to $1.3\text{--}2.5 \times 10^4$ *K. selliformis* cells, suggesting it as a predominant factor in fish mortality. LC-MS/MS analysis did not detect neurotoxic shellfish toxins (BTX2, BTX3), diarrhetic shellfish toxins (DTX1-2, OA), or SPX1. However, gymnodimine-A (GYM-A), a "fast-acting" toxin known to be exclusively produced by *K. selliformis*, was detected at $2.2\text{--}2.5$ pg GYM-A cell⁻¹. To our knowledge, this study represents the first recorded fish-killing caused by a *K. selliformis* bloom in Chinese waters. The study provides the first biological and toxicity insights into *K. selliformis* bloom, crucial for the management and mitigation of fish-killing events associated to harmful algal blooms (HABs) in the Beibu Gulf and the South China Sea.

KEYWORDS

Karenia, phylogeny, hemolytic toxicity, gymnodimine, amplicon sequence variant, harmful algal blooms, Beibu Gulf

1 Introduction

The marine unarmored dinoflagellate *Karenia* is notorious for causing mass mortality of marine organisms and producing over 130 potentially toxic metabolites, including the potent neurotoxic brevetoxins and aerosols (Hort et al., 2021; Natsuike et al., 2023). *Karenia* is widely distributed across global marine waters, however, blooms predominantly occur in East Asia (China, Japan, and Russia), the Mediterranean Sea (Tunisia), the Arabian Sea (Kuwait and Iran), New Zealand, and Chile (Heil et al., 2001; Feki et al., 2013; Li et al., 2019; Iwataki et al., 2022; Orlova et al., 2022; Rolton et al., 2022; Dolatabadi and Attaran-Fariman, 2024). To date, a total of 11 species have been described (Cen et al., 2024; Guiry and Guiry, 2025).

In Chinese waters, eight *Karenia* species have been recorded, including *K. bicuneiformis*, *K. hui*, *K. longicanalis*, *K. mikimotoi*, *K. papilionacea*, *K. brevis*, *K. brevisulcata*, and *K. selliformis* (Cen et al., 2024). However, blooms have commonly been attributed to *K. mikimotoi*, which is ranked as the second most prominent harmful algal bloom (HAB)-causing species, only after *Prorocentrum donghaiense* (syn. *P. obtusidens*), with over 100 blooms reported between 2006 and 2018 in Chinese waters (Li et al., 2017; Lü et al., 2019). Notably, *K. mikimotoi* is recognized as the most deleterious HAB species in terms of economic losses due to fish and shellfish mortality along the Chinese coasts, particularly in the Pearl River Estuary, the East China Sea, and the Changjiang River Estuary (Gu et al., 2022). It accounts for 65.2% of fisheries damage associated with HAB species in China (Sakamoto et al., 2021).

The Beibu Gulf is a semi-enclosed bay in the northwestern South China Sea, characterized by an average annual seawater temperature of 24.5°C and a tropical monsoon climate, with prevailing southwest winds in summer and northeast winds in winter (Xu et al., 2019) (Figure 1). Unlike the South China Sea near Guangdong Province, the

East China Sea, the Yellow Sea, and the Bohai Sea, where various red, brown, green, and golden HABs, including *Karenia*, have frequently occurred since the 1990s (Yu et al., 2023), the Beibu Gulf has long been regarded as the last “clean ocean” in Chinese coastal waters. Therefore, it played a vital role in supporting marine aquaculture in China. The situation changed in January 2015, when the haptophyte *Phaeocystis globosa* bloomed massively in the Beibu Gulf, and even blocked the cooling water supply for a nuclear power station in Fangcheng (Xu et al., 2019). Since then, *Phaeocystis globosa* has become the dominant HAB species in the region, and studies have since been conducted, focusing on its origin, outbreak mechanisms, and modified clay flocculation control strategies (He et al., 2021; Niu et al., 2022; Ren et al., 2022; Li et al., 2024). Dinoflagellate HABs have been rarely recorded over the past decades in the Beibu Gulf (Su et al., 2022).

However, on August 2, 2023, a *Karenia* sp. bloom was documented for the first time near Lianzhou Bay and Tieshan Bay, coinciding with mass mortality of cultured *Trachinotus ovatus* (common name golden pompanos) at the bloom sites, an event unprecedented in the Beibu Gulf in recent decades. This study aims to identify the causative organism through a combination of traditional microscopic observation, molecular marker cloning, and metabarcoding analysis, as well as to determine the potential environmental drivers of the bloom and investigate the association between *Karenia* cell toxicity and fish mortality.

2 Materials and methods

2.1 Study area and sample collection

On August 2, 2023, surface seawater samples were collected from the Beihai aquaculture area in the Beibu Gulf, China, following

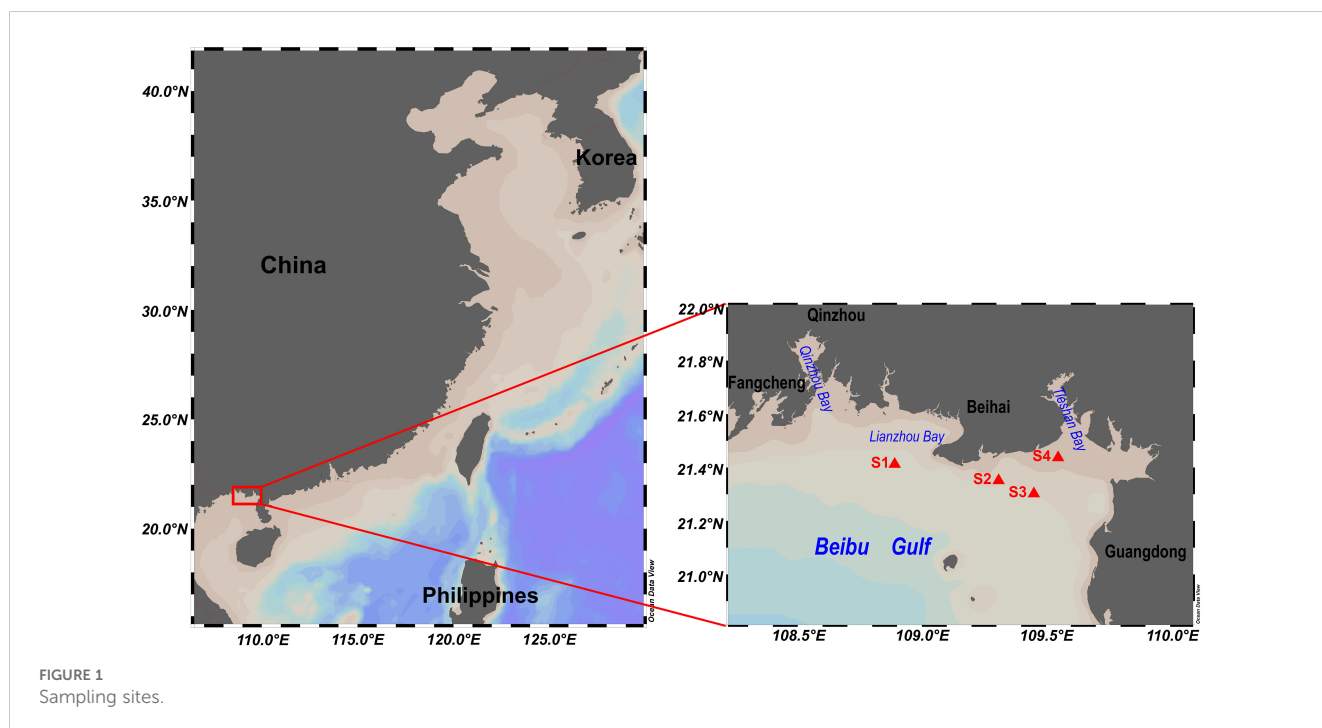


FIGURE 1
Sampling sites.

an incident of *Trachinotus ovatus* mortality (Figure 1). Zooplankton were initially removed using a 160 μm net. A 1000 mL aliquot was fixed with formaldehyde to a final concentration of 2% for microscopic quantification of phytoplankton. The 0.2–160 μm fraction was collected using 0.2 μm GF/C membranes (Cytiva, Massachusetts, USA) and subjected to the cloning of dominant microalgae species and high-throughput sequencing of the variable region 4 of the eukaryotic 18S rDNA (18S rDNA V4) ($n=3$). Additionally, a total of 2250 mL, 4000 mL, and 4000 mL of seawater from sites S1, S2, and S4, respectively, were filtered using 1.2 μm GF/C membranes (Cytiva, Massachusetts, USA) for hemolytic toxicity testing and high-performance liquid chromatography coupled with tandem mass spectrometry (LC-MS/MS) toxin analyses. Hemolytic toxicity and toxin LC-MS/MS analysis at site S3 was not assessed due to sample loss.

2.2 Environmental parameters

Seawater environmental parameters, including pH, dissolved oxygen (DO), dissolved inorganic nitrogen (DIN), phosphate (PO_4^{3-}), chlorophyll-a (Chl-a), and heavy metals (Supplementary Table S1), were measured following the Specification for Marine Monitoring of China (GB17378.1-2007) (General Administration of Quality Supervision et al., 2008). Seawater quality was assessed based on Chinese seawater quality standards (National Environmental Protection Agency, 2004), which classify seawater into four categories (Class I–IV) according to marine functional uses and protection objectives. Class I represents the highest quality, suitable for marine fisheries, nature reserves, and habitats of rare and endangered marine species (National Environmental Protection Agency, 2004). Physical environmental elements, including sea surface temperature (SST), sea surface currents, wind speed, and Chl-a were obtained from Level 4 products of the EU Copernicus Marine Environment Monitoring Service (<https://data.marine.copernicus.eu>). SST had a spatial resolution of $0.05^\circ \times 0.05^\circ$ and a daily temporal resolution. Sea surface currents ($0.25^\circ \times 0.25^\circ$) were derived from geostrophic current fields based on sea level anomalies (SLA) observed by satellite altimeters. Wind speed ($0.125^\circ \times 0.125^\circ$, hourly) was averaged daily for visualization. Chl-a (4 km \times 4 km, daily) was used to represent primary productivity.

2.3 Phytoplankton microscopic counting and molecular marker analyses

Formaldehyde-preserved seawater samples were concentrated in phytoplankton sedimentation chambers for 24 hours and then counted under a microscope at 400 \times magnification (Ni-U, Nikon, Japan), revealing a high abundance of the *Karenia* cells in the seawater.

To identify the dominant *Karenia* at the species-level, DNA from the 0.2–160 μm fraction was extracted using the BioFastSpin DNA Extraction Kit (Bioer Technology, China) following the manufacturer's protocol. The ITS sequences and D1-D3 LSU

rDNA were amplified using the primer pairs ITSA/ITSB (5'-CCTCGTAAACAAGGHTCCGTAGGT-3'/5'-CAGATGCTTAARTTCAGCRGG-3') (Adachi et al., 1994) and 28S-D1R/D3B (5'-ACCCGCTGAATTTAAGCATA-3'/5'-TCGGAAGGAACAGCTACTA-3') (Scholin et al., 1994; Nunn et al., 1996), respectively. The PCR reaction system and conditions were identical to those described by Xu et al. (2024). The ITS (~600 bp) and D1-D3 LSU rDNA (~1000 bp) PCR products were extracted from agarose gels and purified using the Universal DNA Purification Kit (Tiangen, DP214, China), followed by cloning as described in Xu et al. (2021a). For both ITS and D1-D3 LSU rDNA, six clones from each site (S1–S4) were randomly selected for Sanger sequencing. Six ITS sequences (OR604560–OR604565) and two D1-D3 LSU rDNA sequences (OR604586–OR604587) have been deposited in the National Center for Biotechnology Information (NCBI).

2.4 Amplicon 18S rDNA sequencing and data analysis

The genomic DNA was extracted using the cetyltrimethylammonium bromide method (Allen et al., 2006). To target 18S rDNA V4, the DNA was PCR-amplified using the primer pairs AREuk454FWD1 5'-CCAGCASCYGC GGTAATTCC-3'/TAREukREV3 5'-ACTTTCGTTCTTGATYRA-3' (Stoeck et al., 2010). The sequencing library was constructed using the TruSeq[®] DNA PCR-Free Sample Preparation Kit (Illumina, USA), and sequenced on the Illumina NovaSeq 6000 platform (Novogene, Beijing, China) with paired-end reads of 250 bp in length. Raw reads were processed using Cutadapt v2.8 to remove PCR primer matches and potential artificial leftover sequence segments (Martin, 2011). The DADA2 pipeline v1.18 of the software package (Callahan et al., 2016) implemented in R v4.0.4 (R Core Team, 2024) was applied to conduct 3'-end trimming, error filtering, sequence denoising, paired-end reads merging, chimera detection and removal, and the determination and annotation of Amplicon Sequence Variants (ASVs). The 18S sequencing reads were analyzed using the following parameters: maxEE = c (2.2, 2.1), minLen = 150, truncLen = c (220, 210), minBoot = 70, and minOverlap = 10 bases, and the taxonomy was assigned using the reference database PR2 v5.0.0 (Guillou et al., 2012). ASVs annotated as macroalgae, fungi and metazoans were removed from the dataset. A summary of each filtering process on the sequences is shown in Supplementary Table S2. All raw data have been deposited in the NCBI (Bioproject PRJNA1205743). Twenty-one 18S rDNA V4 ASVs assigned to the genus *Karenia* were also deposited into NCBI (PQ822021-PQ822041).

The ASV table was further analyzed in RStudio v.2024.9.0.375 (Posit team, 2024). Protistan alpha diversity (α -diversity) was determined by calculating Hill numbers using iNEXT v3.0.1 package (bootstrap=100, confidence=0.95), for species richness ($q=0$), the exponential of Shannon's entropy index ($q=1$), and the inverse of Simpson's concentration index ($q=2$), respectively (Chao et al., 2014). To assess sequencing depth, rarefaction and

extrapolation curves based on iNEXT function were plotted using the ggplot2 v3.5.1 package. ANOVA and pairwise t-tests with Bonferroni correction were conducted to assess α -diversity variations within and between sites S1-S4, and were visualized using ggplot2. For compositional analysis, singletons in the ASV table were removed and zero values were replaced using the Count Zero Multiplicative method via the cmultRepl function from the zCompositions v1.5.0-4 package. A Centered Log-Ratio (CLR) transformation was then applied to mitigate the compositional effect of microbiome ASV data. The top ten most abundant protistan taxa were plotted using ggplot2.

For protistan beta diversity (β -diversity) analysis, as the first axis length from the Detrended Correspondence Analysis (DCA) was <3 , Redundancy Analysis (RDA) was applied to assess relationships between ASVs and environmental variables. Environmental metadata (pH, DO, DIN, PO_4^{3-}) were z-standardized, multicollinearity was checked using vif.cca function, and highly collinear variables were removed. ANOVA with 999 permutations ($p=0.05$) was used to test the significance of the RDA analysis. Significant environmental factors were identified using the ordistep function, then the final RDA ordination plot was generated based on protistan CLR-transformed ASVs and these significant environmental factors (pH, DIN). Additionally, treemaps were generated using the treemapify v2.5.6 package to visualize phytoplankton categories and their relative compositions at both the phylum and species levels, based on traditional microscopy counts and 18S rDNA V4 ASVs.

2.5 rDNA phylogenetic analysis

The *Karenia* spp. sequences of ITS, D1-D3 LSU rDNA, 18S rDNA V4 ASVs obtained in this study along with reference sequences from the NCBI were aligned using MAFFT v7.526 (Katoh and Standley, 2013) and trimmed in MEGA v10.1.8 (Kumar et al., 2018). Maximum likelihood (ML) phylogenetic analysis was performed at CIPRES server (Stamatakis, 2014) (<https://www.phylo.org/>), with evolutionary models GTR+G+I, GTR+G, and GTR+G+I applied to ITS, D1-D3 LSU rDNA, and SSU sequences, respectively. Evolutionary models for Bayesian inference (BI) phylogenetic analysis were selected using jModelTest 2 v0.1.11 (Guindon and Gascuel, 2003; Darriba et al., 2012). The BI phylogenetic tree was conducted using MrBayes v3.2.7 (Ronquist et al., 2012), with the evolutionary models TIM3+G, TrN+G+I, and TIM1+G selected for the respective datasets. Bayesian analysis was performed in two independent runs, each consisting of four Markov chains and a temperature constant of 0.2. The analysis was run for 5 million generations, sampling every 100 generations, with convergence diagnostics calculated every 1000 generations. The first 25% of samples were discarded as burn-in. The phylogenetic trees were edited in FigTree v1.4.4 and Adobe Illustrator 2020 v24.1.1.

To infer the genealogical relationships among 21 ASVs annotated as *K. selliformis*, a phylogenetic haplotype network using the TCS network method was constructed in PopART v1.7 (<http://popart.otago.ac.nz>) (Leigh et al., 2015).

2.6 Toxin analysis

2.6.1 Hemolytic toxicity

The assay followed the protocol of Song et al. (2023). Briefly, GF/C membranes containing phytoplankton cells were dissolved in 8 mL of rabbit erythrocyte lysis assay (ELA) buffer, and ultrasonically disrupted in an ice bath. The hemolytic toxin extract in the supernatant was collected by centrifugation. For hemolytic toxicity measurement, 1 mL of hemolysin extract was incubated with 1 mL of 5×10^7 cells mL^{-1} rabbit erythrocyte solution as the test sample (A_s). Three controls were included: 1 mL erythrocytes + 1 mL ELA buffer (background), 1 mL hemolysin extract + 1 mL ELA buffer (negative control), and 1 mL erythrocytes + 900 μL ELA buffer + 100 μL TritonX-100 (positive control). All mixtures were incubated at 20°C under a light intensity of 50 $\mu\text{mol m}^{-2}\text{s}^{-1}$ for 5 h, followed by centrifugation at 2000 g, 4°C for 5 min. A 200 μL aliquot of the supernatant was loaded into a 96-well microplate, and absorbance was measured at 414 nm using a microplate reader (Infinite M1000 Pro, Tecan, Switzerland). Here, the hemolytic toxicity was calculated according to Ling and Trick (2010):

$$\% \text{ Hemolytic toxicity} = \frac{A_s - A_b - A_n}{A_p} \times 100 \%$$

Where A_s , A_b , A_n , and A_p represent the absorbance at 414 nm for phytoplankton cells from bloom seawater, background, negative and positive control, respectively. Therefore, the hemolytic toxicity here represented the percentage of hemolytic toxicity caused by the one-eighth (1/8) of total phytoplankton cells on the GF/C membrane to 5×10^7 rabbit erythrocyte cells.

2.6.2 LC-MS/MS

GF/C membranes containing phytoplankton cells were immersed in 5 mL of 50% methanol solution. The mixture was vortexed for 10 min, subjected to ultrasonic extraction for 15 min (JP-060S, Skymen, China), and centrifuged at 4000 g for 10 min. The supernatant was collected and filtered through a 0.22 μm organic nylon membrane (Tianjin Navigator Lab Instrument Co., Ltd, China) and further analyzed for toxin profiles using LC-MS/MS (Agilent 1260-6460, California, USA). The analyzed toxins included BTX-2, BTX-3, GYM-A, and SPX1 (ESI+ mode), as well as DTX1, DTX2, and OA (ESI- mode). Standards for DTX1, DTX2, GYM-A, OA, and SPX1 were purchased from the National Research Council, Canada. However, standards for BTX-2 and BTX-3 were unavailable. BTX-2 was characterized by m/z 895.5/877.5 and 895.5/859.6, and BTX-3 was identified by m/z 897.5/807.7 and 897.5/725.2, respectively.

The liquid chromatography was performed using an Agilent InfinityLab Poroshell 120 EC-C18 column (4.6×150 mm, 4 μm) with an injection volume of 10.0 μL . The mobile phase A consisted of 5 mmol/L ammonium acetate in 0.1% formic acid aqueous solution, while mobile phase B was acetonitrile. The column temperature and flow rate were set to 40.0°C and 0.8 mL min^{-1} for ESI+ mode, and 30.0°C and 0.6 mL min^{-1} for ESI- mode, respectively. Mass spectrometry was performed using electrospray

ionization (ESI) as the ionization source, with a sheath gas temperature of 350°C and a flow rate of 11 L min⁻¹. The nozzle voltage was set to 500 V, the capillary voltage to 4000 V, and analysis was conducted in Multiple Reaction Monitoring (MRM) mode. In ESI+ mode, the nebulizer pressure was 45 psi, and the dry gas flow rate was 5 L min⁻¹. In ESI- mode, these values were 50 psi and 10 L min⁻¹, respectively. The gradient elution program and MRM parameters for LC-MS/MS were listed in [Supplementary Table S3](#).

3 Results

3.1 Environmental factors

Based on the *Karenia* cell concentration and fish mortality, the study period was divided into three phases: before the bloom (August 1, 2023), during the bloom (August 2, 2023), and after the bloom (August 3–4, 2023). Mortality of cultured *Trachinotus ovatus* was observed only on August 2, 2023, near Lianzhou Bay and Tieshan Bay in the Beibu Gulf, coinciding with the occurrence of a *Karenia* bloom ([Figure 1](#)). During the bloom, the water condition at sampling sites S1–S4 was good and classified as Class I according to Chinese seawater quality standards ([National Environmental Protection Agency, 2004](#)) ([Supplementary Table S1](#)). Therefore, fish mortality resulting from heavy metal contamination or general water pollution was ruled out.

Satellite data indicated that from August 1 to 4, 2023, sea surface temperature remained steady at 31.1–31.3°C ([Figure 2](#); [Supplementary Figure S1](#)). Before and during the bloom (August 1–2), relatively weak westward sea surface winds facilitated the convergence of offshore and within the bay microalgae, including *Karenia*, toward the coast and small embayments via Ekman transport. After the bloom (August 3–4), sea surface winds intensified and shifted to a southwestern direction ([Figure 2](#); [Supplementary Figure S1](#)). In response to these winds, sea surface currents flowed westward along the northern coast of the Beibu Gulf, potentially transporting phytoplankton from eastern to western part of Qinzhou and Fangcheng ([Figure 2](#); [Supplementary Figure S1](#)). Additionally, sea level anomaly data revealed clear Kelvin wave propagation from east to west along the coast ([Figure 2](#)). Together, these physical environmental factors supported the occurrence of elevated Chl-*a* concentrations westward along the coast from August 1 to 4, 2023 ([Figure 2](#); [Supplementary Figure S1](#)).

3.2 Protistan community characteristics

The average raw read counts for 18S rDNA V4 were 140,528. After denoising, low-quality read removal, and chimera elimination, an average of 83.5% of the raw reads remained for further analysis ([Supplementary Table S2](#)). The rarefaction/extrapolation curves for 18S rDNA V4 ($q = 0$, $q = 1$, $q = 2$) plateaued, indicating that the sequencing depth was sufficient to reliably capture protistan community composition and diversity

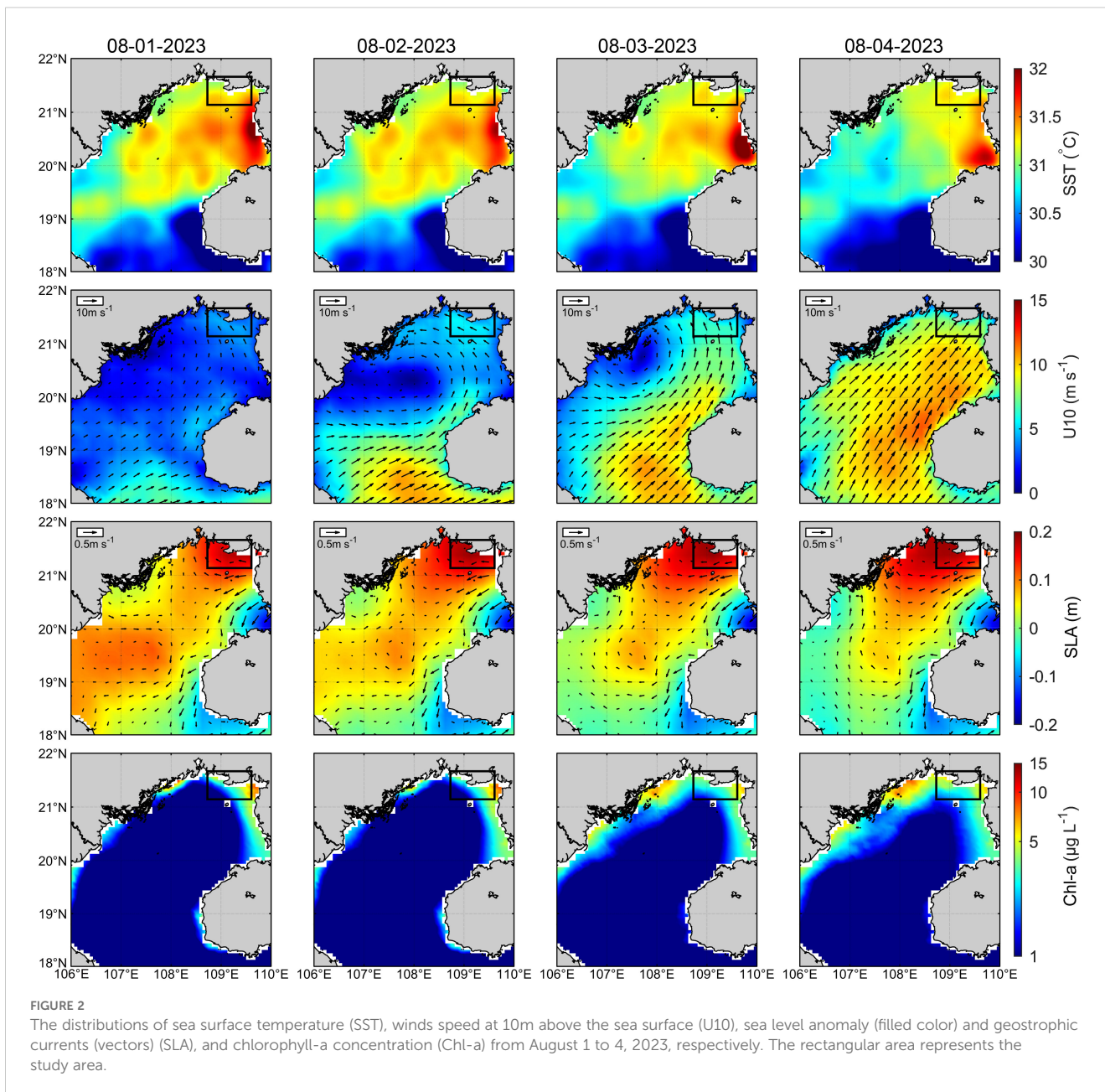
([Supplementary Figure S2](#)). In the bloom seawater, the most abundant protists were Dinoflagellata (42.6%) and Gyrista (20.6%) at the division level; Dinophyceae (28%), Syndiniales (14.7%), and Mediophyceae (9.3%) at the class level; and Dino-Group-II (12.3%) and Gymnodiniales (8.6%) at the order level ([Supplementary Figure S3](#)). MOCH-5_XXX (2.9%) and *Gyrodinium* (2.7%), and MOCH-5_XXX.sp. (3.3%) and Dino-Group-II-Clade-1_X.sp. (2.3%) corresponded to the most abundant genera and species, respectively. The bloom causative organism *Karenia* generally occupied 1.2% and 1.4% at the genus and species levels, respectively.

Both protist richness and evenness varied significantly among the four sites ($p < 0.01$), with richness at S2–S4 significantly higher than at S1, and evenness at S4 significantly greater than at S1–S3 ([Supplementary Figure S4](#)). The RDA analysis revealed that the RDA1 and RDA2 axes explained 32.3% and 26.0% of the variation, respectively. Among the environmental factors, pH and DIN were the primary drivers of community distribution, accounting for 58.3% of the total variation ([Figure 3](#)). The remaining RDA axes added another 1.8% to the constrained variance, while the remaining 39.9% was attributed to unconstrained factors. Site S1 was primarily influenced by pH, while S4 was driven by DIN. Sites S2 and S3 were less affected by pH and DIN, clustering closely and exhibiting more similar protist community composition compared to S1 and S4 ([Figure 3](#)). The genera *Chlorodendrales_XX*, *Acanthometra*, and *Grammatodinium* were positively correlated with pH and predominantly distributed at S1, while the genus *Urgorri* was positively correlated with DIN and mostly distributed at S4. The genus *Peronosporomycetes_XXX* ordinated between Site 1 and Site 4 ([Figure 3](#)).

3.3 Phytoplankton community characteristics

The phytoplankton composition, determined by microscopic counting and 18S rDNA V4 ASVs showed substantial agreement, with both methods identifying Heterokontophyta and Dinoflagellata as the dominant phyla. These phyla accounted for 62.4% and 33.7% in microscopic counts, and 37.3% and 43.9% in ASV sequences, respectively ([Figure 4](#); [Supplementary Table S4](#)). However, microscopic counting uniquely identified Cyanophyta, Euglenophyta, and Xanthophyta, whereas ASVs exclusively detected Haptophyta, Prasinodermophyta, and Rhodophyta ([Figure 4](#)). At the species level, microscopic counting identified 86 species, obviously fewer than the 171 species detected through ASVs. The bloom-forming organism, *Karenia* sp., accounted for an average of 32.6% of the total phytoplankton abundance in S1–S4 based on microscopic counts but only 3.1% in ASV-based estimates ([Figure 4](#)). Nevertheless, *Karenia* sp. was among the most abundant phytoplankton ASVs, alongside *Spiniferites mirabilis* (4.2%), *Oodinium pouchetii* (4.0%), and Dinophyceae_XXX.sp. (3.4%).

Karenia sp. was the most abundant species at S1, S2, and S3, contributing 91.3%, 70.5%, and 38.3% of the total abundance in microscopic counts, respectively. At S4, *Skeletonema tropicum*



dominated, while the abundance of *Karenia* sp. ranked third, accounting for 7.5%. Despite these composition differences, the cell density of *Karenia* sp. remained within the same order of magnitude across S1–S4, with 8.9×10^4 , 4.9×10^4 , 1.4×10^4 , and 2.7×10^4 cells L^{-1} , respectively (Figure 5; Supplementary Table S4). The ASV abundance of *Karenia* sp. in S1–S4 remained relatively constant ranging from 13.9 (S1) to 19.6 (S3) in CLR-normalized values, accounting for 2.6% (S4) to 3.9% (S1) of the total ASV abundance (Figure 5).

3.4 Phylogenetic analysis of *Karenia*

The six ITS clone sequences and two D1-D3 LSU rDNA clone sequences were 676 bp and 1,042 bp in length, respectively, while

the twenty-one 18S rDNA V4 ASV sequences ranged from 340 to 412 bp, with an average length of 378 bp. After trimming and alignment, the sequence lengths used for ITS, D1-D3 LSU rDNA, and SSU phylogenetic analyses were 658 bp, 897 bp, and 1,667 bp, respectively. The tree topologies generated by ML and BI analyses are mostly consistent, and the ML tree is presented here. The phylogenetic tree showed that both ITS clones BGERL260–BGERL265 and D1-D3 LSU rDNA clones BGERL266–267 clustered with strains of *K. selliformis*, supported by high bootstrap and posterior probability values of 88/1.0 and 98/1.0, respectively (Figure 6; Supplementary Figure S5). In the SSU phylogenetic tree, all 21 ASVs also clustered exclusively with *K. selliformis* strain CAWD79 (Figure 7).

Phylogenetic haplotype networks revealed notable genetic diversity among the 21 ASVs annotated as *K. selliformis*, with a

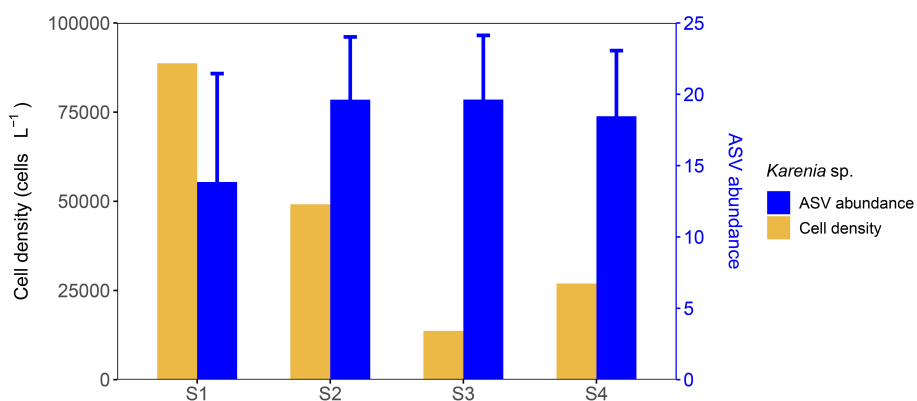


FIGURE 5
Karenia sp. cell density from microscopic counts and ASV relative abundance after CLR-normalized transformation.

3.5 Toxin analysis

Phytoplankton cells collected by filtration from 2250 mL, 4000 mL, and 4000 mL of seawater at sites S1, S2, and S4, respectively, were analyzed for hemolytic toxicity using rabbit erythrocytes.

Combing the microscopic cell density for *Karenia* sp., 88,690, 49,143, and 26,931 cells L⁻¹ and the molecular identification of bloom causative organism as unique *K. selliformis* (see 3.3 and 3.4), 1/8 of the total *K. selliformis* cell numbers were calculated as 2.5×10^4 from S1, 2.5×10^4 from S2, and 1.3×10^4 from S4, and exhibited

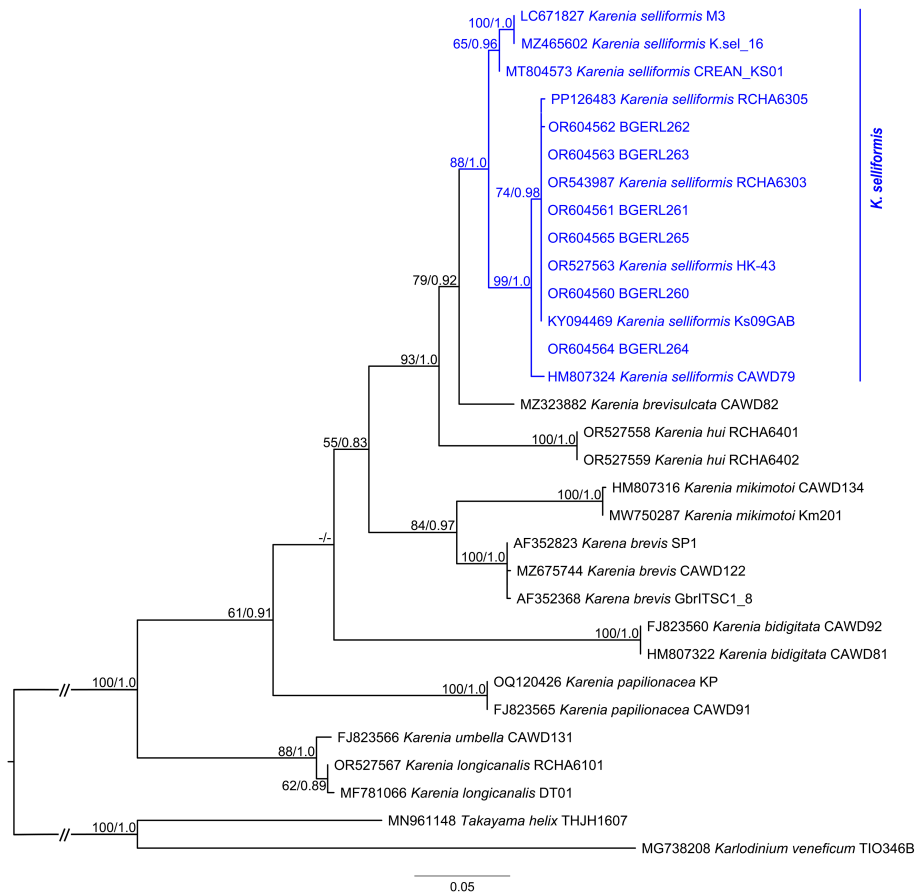
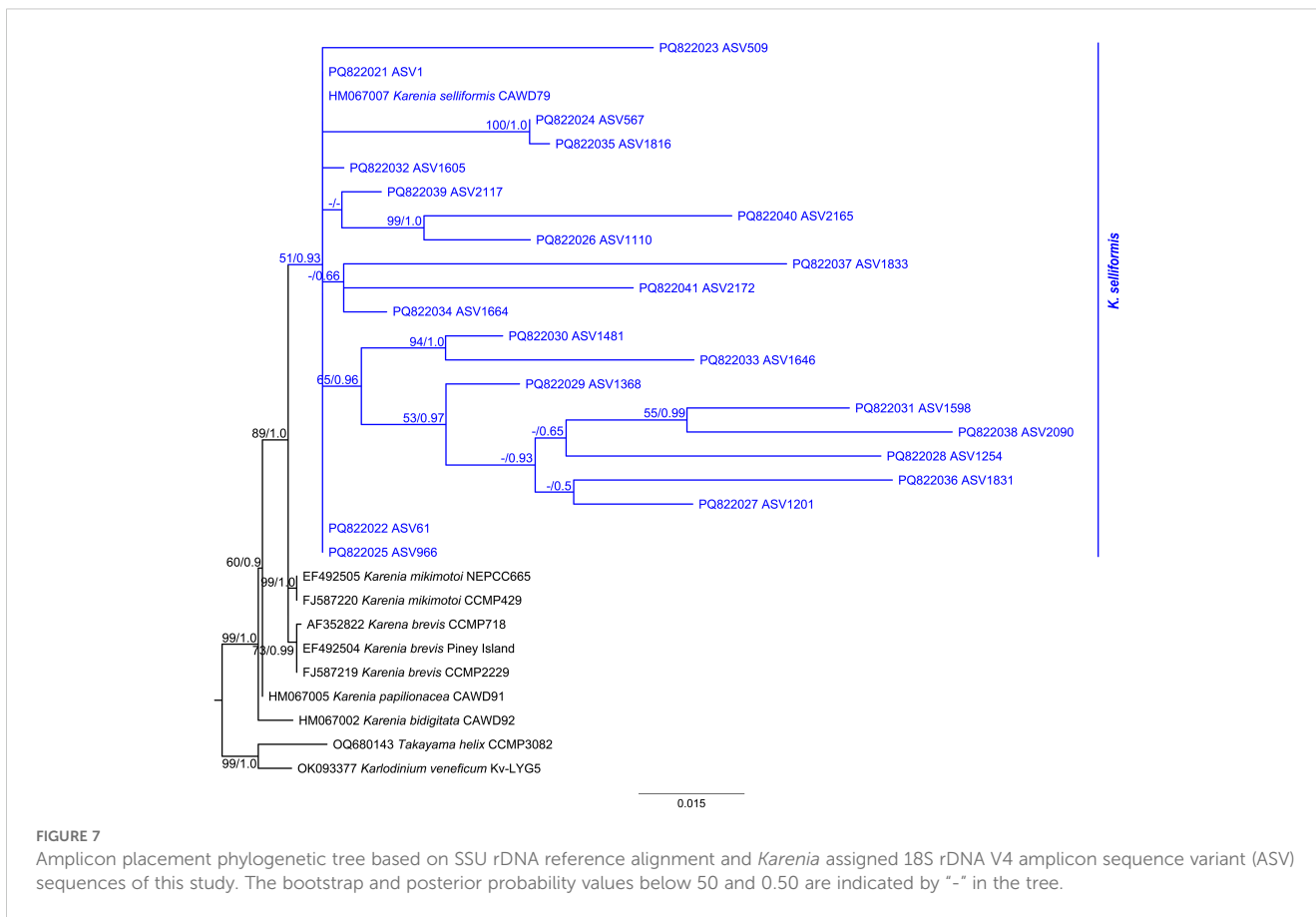


FIGURE 6
 Phylogenetic tree based on ITS sequences. The bootstrap and posterior probability values below 50 and 0.75 are indicated by “-” in the tree.



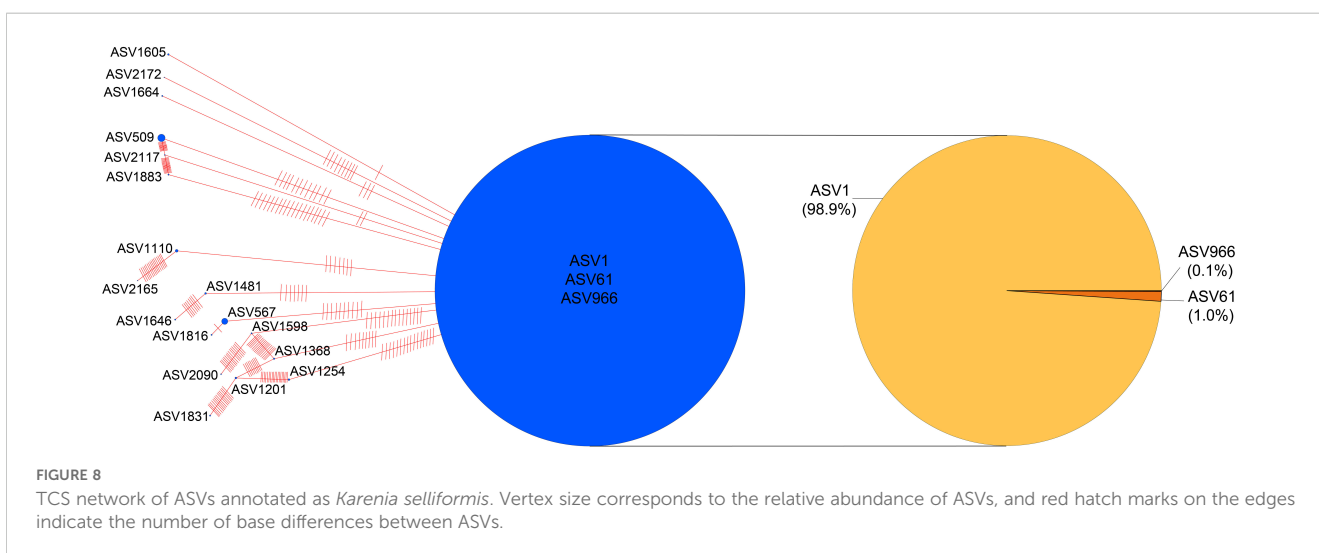
hemolytic toxicities of 48.3%, 47.6%, and 45.2% to 5×10^7 rabbit erythrocyte cells, respectively.

In the LC-MS/MS analysis, BTX2, BTX3, DTX1-2, OA, and SPX1 were not detected. However, GYM-A was detected at all three sites (Figure 9). According to previous research, GYM-A is exclusively produced by *K. selliformis* (Hort et al., 2021; Wu et al., 2024). Therefore, *K. selliformis* from S1, S2, and S4 generated GYM-A contents of 2.3, 2.5, and 2.2 pg cell^{-1} , respectively.

4 Discussion

4.1 Confirmation of *K. selliformis* as HAB causative organism

In this study, light microscopy identified *Karenia* sp. as the dominant species. However, the small cell size and the highly similar morphology within the genus made species-level



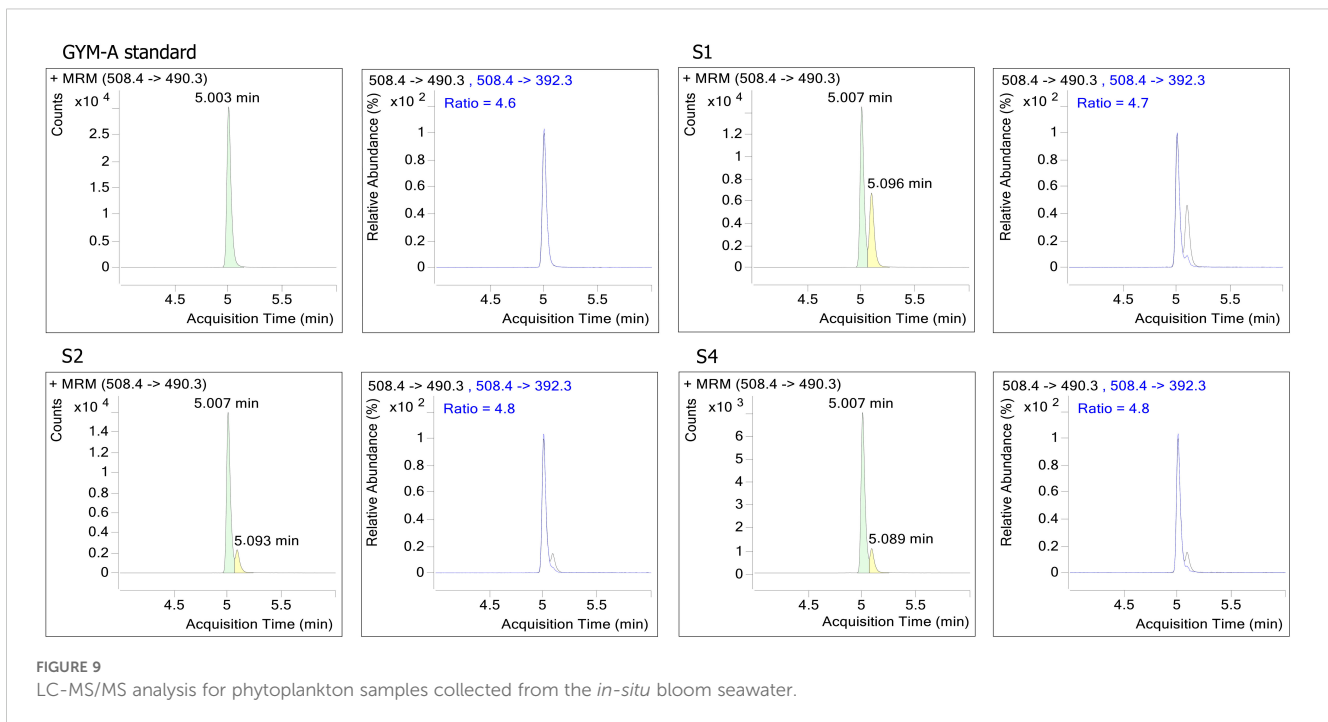


FIGURE 9
LC-MS/MS analysis for phytoplankton samples collected from the *in-situ* bloom seawater.

identification challenging, especially given previous reports of the frequent coexistence of multiple *Karenia* species, along with other morphologically similar members of Kareniaceae, such as *Karodinium* and *Takayama*, within the same bloom (Wolny et al., 2015; Orlova et al., 2022). The species from the *in-situ* bloom waters was successfully identified as *K. selliformis* based on the molecular cloning approach and sequencing of ITS (six) and D1-D3 LSU rDNA (two) clones. Phylogenetic trees supported the previous finding that this species can be divided into at least two phylotypes (Iwataki et al., 2022; Orlova et al., 2022; Cen et al., 2024), with ITS and D1-D3 rDNA sequences from this study grouped in the same phylotypes with those from South China Sea (Figures 6, 7; Supplementary Figure S5). The SSU rDNA tree topology further indicated that only *K. selliformis* has been found within all the twenty-one 18S rDNA V4 ASVs assigned to the genus *Karenia*. In addition, GYM-A was the only lipophilic toxin detected in the *in-situ* bloom water, which so far can only be produced by the dinoflagellate *K. selliformis* (Hort et al., 2021; Wu et al., 2024). The combination of the dominance of *K. selliformis* and GYM-A detection strongly suggest that *K. selliformis* is the causative organism for this harmful bloom event.

To the best of our knowledge, this is the first recorded *K. selliformis* bloom in Chinese waters. Although *Karenia* species are among the most detrimental HAB-causing organisms and frequently bloom across Chinese seawaters from north to south, their blooms have typically been attributed to *K. mikimotoi* (Li et al., 2019). *Karenia selliformis* was first identified in New Zealand and initially referred to as *Gymnodinium* sp. by Mackenzie et al. (1996). Later, Haywood et al. (2004) formally described the species *K. selliformis* using strain CAWD79 from Foveaux Strait, South Island, New Zealand. This species has caused blooms in Kuwait, Iran, New Zealand, Chile, Tunisia (Seki et al., 1995; Heil et al., 2001; Feki et al.,

2013; Mardones et al., 2020; Baldrich et al., 2024; Dolatabadi and Attaran-Fariman, 2024), especially become serious in last years in East Asia waters (Russia, Japan), resulting in mass mortality of marine fauna in the region (Orlova et al., 2022; Takagi et al., 2022). In Japan, the economic loss caused by *K. selliformis* in Hokkaido in 2021 has exceeded the largest record set by the *Chattonella* bloom in the Seto Inland Sea in 1972 (Iwataki et al., 2022).

As a country heavily impacted by HABs since the 1990s, it is not surprising that China now records a *K. selliformis* bloom. In China, *K. selliformis* was firstly reported in 2016 during a *K. mikimotoi* dominant bloom in Tolor Harbor, Hong Kong, along with cells of *K. longicanalis*, *K. papilionacea*, and *K. selliformis* (Lin et al., 2020). Subsequently, more strains of *K. selliformis* were isolated from the South China Sea between 2021 and 2023, including the central Beibu Gulf in August 2023 (Cen et al., 2024). This occurred nearly two decades after the first large-scale *K. mikimotoi* bloom in the Zhujiang Estuary in 1998 (Li et al., 2019). However, recent studies on *Karenia* genetic diversity using DNA metabarcoding have consistently detected *K. selliformis* from environmental DNA in the East China Sea and South China Sea (Zhang et al., 2022, 2025). Combined with the recent confirmation of resting cysts in species within the genera *Karenia* and *Karodinium* (Liu et al., 2020; Tang et al., 2021a), we speculate that *K. selliformis* should have persisted at low background densities in Chinese waters, including Beibu Gulf, for much longer than previously assumed.

To overcome the challenges of microscopic morphological observation in small and fragile cells, rDNA-based metabarcoding has been increasingly integrated with traditional microscopy in studies of phytoplankton diversity and abundance (Kezlya et al., 2023). This approach has led to the discovery of numerous new HAB species in marine environments (Stern et al., 2010; Cui et al., 2021; Smith et al., 2024). In this study, taxa such as Haptophyta,

Prasinodermophyta, and Rhodophyta were uniquely detected through ASV analysis. However, it is noteworthy that results from metabarcoding and microscopy may differ substantially, especially for dinoflagellates. Dinoflagellates possess exceptionally large genome sizes among eukaryotes (~1–250 Gbp), with high and variable gene copy numbers both within and between species (Casabianca et al., 2017; Lin, 2024). These differences can be further amplified by PCR in metabarcoding approach. It likely accounts for the marked difference in *Karenia* abundance estimates in this study—32.6% by microscopy versus 3.1% by ASV analysis. To mitigate this issue in future work, in addition to 18S rDNA V4 primers, multiple longer or alternative primers targeting more variable regions such as ITS and LSU rDNA should be considered.

4.2 Potential drivers for *K. selliformis* outbreak

HABs in marine ecosystems are complex ecological disasters driven by internal and external factors. Biological characteristics of *K. selliformis* from the Beibu Gulf are currently limited. However, evidence from its bloom environmental conditions and cultures isolated from distinct regions suggests that *K. selliformis* has high physiological plasticity, enabling it to thrive across diverse marine environment (Medhioub et al., 2009; Vellojin et al., 2023). Blooms of *K. selliformis* have been documented across a range of temperatures, including 13.5–15°C in temperate waters of the Southern Pacific (42–53°S) (Clément et al., 2000; Uribe and Ruiz, 2001; Guillou et al., 2002; Mardones et al., 2020) and 7–23°C in temperate waters of the Northwestern Pacific (43–56°N) (Iwataki et al., 2022; Orlova et al., 2022). In subtropical Arabian waters (25° N), blooms have been reported at 25–28.6°C (Heil et al., 2001; Dolatabadi and Attaran-Fariman, 2024), while in this study, *K. selliformis* bloom was observed at 31°C in the tropical Beibu Gulf (21°N), pushing the upper limit of previously reported temperature regimes. The species has also bloomed across a wide salinity range of 20–50 in various water bodies (Medhioub et al., 2009; Feki-Sahnoun et al., 2017; Li et al., 2018; Guangxi Marine Bureau, 2023; Vellojin et al., 2023). In contrast, pH fluctuations during blooms tend to be narrower, mostly around 8.0 as the general seawater value. However, in laboratory experiment, *K. selliformis* can grow within a broad pH range of 7.0–9.0 (Vellojin et al., 2023). The increased pH values measured at field site S1 is in alignment with high Chl-a values and high photosynthetic rates reduce the CO₂ and hence increases the pH in the water (Supplementary Table S1). In this study, nutrient levels including DIN and PO₄³⁻ were low, with water quality classified as Class I. However, as the genus *Karenia* is mixotrophic, capable of utilizing a wide range of inorganic and organic nutrient sources (Li et al., 2019; Ahn and Glibert, 2024), nutrient availability is unlikely to have limited its outbreak in the Beibu Gulf, rather might be the mixotrophic an competitive advantage for the species in low nutrient environments. However, not all *Karenia* species are mixotrophic (Ok et al., 2023), and further study is needed to understand the nutritional acquisition strategy of *K. selliformis* in the Beibu Gulf.

In addition to the favorable marine environment supporting *K. selliformis* cell accumulation and maybe even growth in the Beibu Gulf, the bloom was also driven by physical factors, particularly sea surface wind. The weak westward onshore sea surface winds before and during the bloom on August 1–2, 2023 produced a stable water environment, which is favorable for unarmored dinoflagellates, such as *Karenia*, as they possess delicate cell structures due to the lack of cellulose thecae, highlighting their preference for low-disturbance environments (Brand et al., 2012; Stumpf et al., 2022). While onshore sea surface wind may drive the seawater towards shoreline and cause cell accumulation near coast. A similar phenomenon was found during the large-scale *K. mikimotoi* bloom along the Fujian coast in May–June 2012, when the northerly onshore winds accumulated water towards nearshore, and provide a stable hydrodynamic environment conducive to cell division and bloom formation (Deng et al., 2016). The unprecedented *K. selliformis* bloom in eastern Hokkaido, Japan, during autumn 2021, was also associated with southerly wind-driven current, which resulted in transportation of offshore water towards the shoreline, causing bloom outbreak and prolong due to algal accumulation in the semi-closed fishing port (Hasegawa et al., 2022). In this study, the strong southwest winds on August 3–4, following the bloom, contributed to the degradation of *K. selliformis* in Lianzhou Bay and Tieshan Bay, which is a common factor in HAB decline (Li et al., 2023).

The westward wind and currents most likely transported cells of *K. selliformis* from Lianzhou Bay and Tieshan Bay westward along the coastline, which explains the *Karenia* outbreak in Fangcheng coastal waters on August 7, 2023, with cell density ranging from 2.3–9.7×10⁴ cells L⁻¹, as well as scattered dead fish floating on the sea surface (Guangxi Marine Bureau, 2023). Similar to this study, seawater pH, DO, chemical oxygen demand, DIN, PO₄³⁻, Chl-a concentrations in Fangcheng waters were all within the typical range for the region, with most indices belonging to water quality class I (Guangxi Marine Bureau, 2023). The government reported *Karenia* cells as *K. mikimotoi*, possibly based on microscopic observation (Guangxi Marine Bureau, 2023). However, we speculate that the cells were actually *K. selliformis*, particularly given that *K. mikimotoi* has not been detected so far in the Beibu Gulf, even using DNA metabarcoding technology, neither through ASV analysis in this study, nor via the Operational Taxonomic Unit analysis in Li (2022).

4.3 Possible causes for cultured fish mortality

Fish mortality is the most common and devastating consequence of *Karenia* blooms, primarily attributed to gill damage caused by the hemolytic toxicity of *Karenia* cells (Li et al., 2019; Sakamoto et al., 2021). This toxin can lyse blood cells in the gills, trigger excessive mucus, entangle gill filaments, and ultimately lead to fish suffocation. Hemolytic toxins are not a single specific compound but a group of components, only some of which have been identified, such as all-cis-3,6,9,12,15-octadecapentaenoic

acid, monogalactosyl diacylglycerol, and digalactosyl diacylglycerol (Brand et al., 2012; Li et al., 2019). Although in this study, some other potential fish-killing algal organisms, like *Akashiwo sanguinea*, *Alexandrium leei*, *Margalefidinium fulvescens* (Gu et al., 2022), were also detected, their abundance/reads is negligible comparing to *K. selliformis* (Supplementary Table S4). As all tested field samples exhibited strong hemolytic activity (45.2%–48.3%), it supports hemolytic toxicity produced by *K. selliformis* is responsible for the cultured *Trachinotus ovatus* mortality during the bloom in the Beibu Gulf.

Karenia selliformis generally has stronger hemolysis and cytotoxicity than other *Karenia* species. Among the four *Karenia* species from Hong Kong blooms in 2016, *K. selliformis* (strain CCHA-7) had lower hemolytic toxicity (42.3%) than *K. longicanalis* (46.4%), but higher than *K. mikimotoi* (37.8%) and *K. papilionacea* (37.0%) (Lin et al., 2020). Both cells and culture media of *K. selliformis* culture (CAWD79, New Zealand) consistently contained hemolytic activity, with mean hemolytic toxicity of 10^2 relative to *K. brevis* (Tatters et al., 2010). In gill cell-based assay, *K. selliformis* (CREAN-KS00, Chile) was highly cytotoxic to reduce gill cell viability down to 28.3–44.7% of controls by supernatant and lysed cell suspensions (Mardones et al., 2020). Similarly, *K. bicuneiformis* can be prey for common heterotrophic dinoflagellates, whereas *K. selliformis* (NIES 4541, Japan) lyse all predator (Park et al., 2024). The high potential of *K. selliformis* to exert toxic effects on marine organisms within the ecosystem has also been documented. The Hokkaido *K. selliformis* (Ks-01) could markedly decrease the survival and ingestion of copepod, no matter in direct contact, indirect interaction, or ingestion of *K. selliformis* (Ohnishi et al., 2024). During the interaction between calanoid copepod *Acartia hongii* and *Karenia*, Ok et al. (2024) concluded *K. selliformis* (NIES-4541, Japan) had almost the highest mortality to copepod at similar dinoflagellate concentrations, and the lowest ingestion rate among *A. hongii* feeding on harmful dinoflagellates. *K. selliformis* strain obtained from the South China Sea had much stronger acute toxicity to rotifer *Brachionus plicatilis* than *K. umbella*, with LD50 (lethal dose fifty) $2,750 \text{ mL}^{-1}$ vs. $14,011 \text{ mL}^{-1}$ (Li et al., 2018). Among the five Chinese *Karenia* species, *K. hui*, *K. longicanalis*, *K. mikimotoi*, *K. papilionacea*, and *K. selliformis*, *K. selliformis* (HK-43, China) showed the strongest acute toxicity on marine model organism of medaka *Oryzias melastigma*, resulting in 100% mortality within 4 h and the most shortest LD50 of 2h (Cen et al., 2024). The simulated food chain from *K. selliformis* (GM94GAB, Tunisia) to brine shrimp and further to marine medaka induced abnormal swimming behavior, pathological damage to the intestine and liver tissues, and energy metabolism disorders in medaka (Liu et al., 2023). Therefore, *K. selliformis* has been proved to be a highly toxic organism, which explains the mass mortality of aquaculture fish in the Beibu Gulf.

4.4 GYM-A produced by *K. selliformis* in the bloom

Besides hemolytic toxicity, GYM-A, a “fast-acting” lipophilic toxin was also detected in field samples in this study, whereas the other

lipophilic toxins, i.e. neurotoxic shellfish toxins (BTX2, BTX3), diarrhetic shellfish toxins (DTX1-2, OA), and SPX1, were not detected. GYM-A belongs to cyclic imines toxins family, initially identified from oyster (*Tiostrea chilensis*) in New Zealand in 1994, and displays toxicity due to its potent antagonists of the nicotinic acetylcholine receptors (Seki et al., 1995; Molgó et al., 2017). GYM-A, along with its analogs GYM-B and GYM-C, is primarily produced by *K. selliformis*, though not all isolates of this species generate GYM-A (Miles et al., 2000, 2003; Mardones et al., 2020). In this study, *K. selliformis* from the bloom in the Beibu Gulf generated 2.2–2.5 pg GYM-A cell⁻¹, which is comparable to a *K. selliformis* strain (GM94GAB) from Tunisia with a range of 1.2–22.4 pg cell⁻¹ (Medhioub et al., 2009), but higher than 0.9 pg cell⁻¹ produced by the strain (HK-43) from Tolo Harbor, South China Sea (Cen et al., 2024). Considering the extraction efficiency of GYM-A, the actual toxin quota collected by filtration in this study may represent only ~34% of the total GYM-A (Tang et al., 2021b), with the residual lost in the water during harvesting process.

The role of GYM-A in the marine species mortality is unclear. Previous studies suggest that the neurotoxicity of *K. selliformis*, due to GYM-A and its analogues, can sensitize marine species to cytotoxins (Dragunow et al., 2005). However, Mardones et al. (2020) pointed out that the massive fauna mortality during *K. selliformis* bloom along the Chilean coast was likely induced by ichthyotoxic polyunsaturated fatty acids and/or uncharacterized toxic compounds, rather than GYMs. As a lipophilic toxin, GYM-A is well-known for its accumulation in shellfish and the potential risks to human health. Both GYM-A and its fatty acid conjugates have been widely detected in various shellfish worldwide (Finch et al., 2024). In China, shellfish with high GYM-A concentrations are primarily found in the South China Sea, particularly in the Beibu Gulf (Ji et al., 2020), which indirectly supports the widespread presence of *K. selliformis* in the region. In this area, GYM-A and SPX1 are the predominant lipophilic phycotoxins in shellfish, with a significant positive correlation observed between GYM-A levels in shellfish and seawater (Xu et al., 2021b; Ji et al., 2022). However, only recently have cultures and environmental DNA analyses confirmed the presence of *K. selliformis* for this toxin in the Beibu Gulf (Li, 2022; Cen et al., 2024). Further research is required to elucidate the role of GYM-A in *K. selliformis* blooms and its impact on aquaculture and other organisms within the ecosystem.

5 Conclusions

This study investigated the first mass fish mortality associated with a *Karenia* bloom in the Beibu Gulf, China. During the bloom, seawater maintained a good quality of Class I. Using a combination of traditional microscopic observation, rRNA gene cloning, and 18S rDNA ASV analysis of *in-situ* bloom samples, *K. selliformis* was identified as the bloom-causing organism. Weak westward sea surface winds before and during the bloom facilitated the accumulation and outbreak of *K. selliformis* in Lianzhou and Tieshan coastal waters, while hemolytic toxicity was the predominant cause of fish mortality. The “fast-acting” toxin of GYM-A was detected, but its role in *K. selliformis* bloom remains unclear. To our knowledge, this study represents the first documented fish-killing event caused by *K.*

selliformis in Chinese waters. Further research on its physiology, toxicity mechanisms, and bloom formation under the background of climate change is essential for understanding its impact on marine aquaculture in the Beibu Gulf.

Data availability statement

The original contributions presented in the study are included in the article/Supplementary Material, further inquiries can be directed to the corresponding author/s.

Ethics statement

Ethical approval was not required for the studies on animals in accordance with the local legislation and institutional requirements because only commercially available established cell lines were used.

Author contributions

YX: Data curation, Formal analysis, Funding acquisition, Methodology, Visualization, Writing – original draft, Writing – review & editing. XW: Data curation, Visualization, Writing – original draft. CH: Data curation, Formal analysis, Methodology, Writing – review & editing. ND: Validation, Writing – review & editing, Methodology. XZ: Methodology, Writing – review & editing. SN: Data curation, Software, Writing – review & editing. MT: Writing – review & editing, Methodology. WL: Funding acquisition, Writing – review & editing, Investigation. UJ: Writing – review & editing, Conceptualization, Funding acquisition, Writing – original draft.

Funding

The author(s) declare that financial support was received for the research and/or publication of this article. This research was

supported by the Natural Science Foundation of Guangxi Province (2020GXNSFDA297001, 2024GXNSFAA010136), the National Natural Science Foundation of China (41976155, 42376211), the Project of Southern Marine Science and Engineering Guangdong Laboratory (Zhuhai) (SML2024SP023), and the scientific research capacity building project for Beibu Gulf Marine Ecological Environment Field Observation and Research Station of Guangxi (Guike23-026-271).

Conflict of interest

The authors declare that the research was conducted in the absence of any commercial or financial relationships that could be construed as a potential conflict of interest.

Generative AI statement

The author(s) declare that no Generative AI was used in the creation of this manuscript.

Publisher's note

All claims expressed in this article are solely those of the authors and do not necessarily represent those of their affiliated organizations, or those of the publisher, the editors and the reviewers. Any product that may be evaluated in this article, or claim that may be made by its manufacturer, is not guaranteed or endorsed by the publisher.

Supplementary material

The Supplementary Material for this article can be found online at: <https://www.frontiersin.org/articles/10.3389/fmars.2025.1582234/full#supplementary-material>

References

- Adachi, M., Sako, Y., and Ishida, Y. (1994). Restriction fragment length polymorphism of ribosomal DNA internal transcribed spacer and 5.8s regions in Japanese *Alexandrium* species (Dinophyceae). *J. Phycol.* 30, 857–863. doi: 10.1111/j.0022-3646.1994.00857.x
- Ahn, S. H., and Glibert, P. M. (2024). Temperature-dependent mixotrophy in natural populations of the toxic dinoflagellate *Karenia brevis*. *Water*. 16, 1555. doi: 10.3390/w16111555
- Allen, G. C., Flores-Vergara, M., Krasynanski, S., Kumar, S., and Thompson, W. (2006). A modified protocol for rapid DNA isolation from plant tissues using cetyltrimethylammonium bromide. *Nat. Protoc.* 1, 2320–2325. doi: 10.1038/nprot.2006.384
- Baldrich, Á.M., Díaz, P. A., Rosales, S. A., Rodríguez-Villegas, C., Álvarez, G., Pérez-Santos, I., et al. (2024). An unprecedented bloom of oceanic Dinoflagellates (*Karenia* spp.) inside a fjord within a highly dynamic multifrontal ecosystem in Chilean Patagonia. *Toxins*. 16, 77. doi: 10.3390/toxins16020077
- Brand, L. E., Campbell, L., and Bresnan, E. (2012). *Karenia*: The biology and ecology of a toxic genus. *Harmful Algae*. 14, 156–178. doi: 10.1016/j.hal.2011.10.020
- Callahan, B. J., McMurdie, P. J., Rosen, M. J., Han, A. W., Johnson, A. J. A., and Holmes, S. P. (2016). DADA2: High-resolution sample inference from Illumina amplicon data. *Nat. Methods* 13, 581–583. doi: 10.1038/nmeth.3869
- Casabianca, S., Cornetti, L., Capellacci, S., Vernesi, C., and Penna, A. (2017). Genome complexity of harmful microalgae. *Harmful algae*. 63, 7–12. doi: 10.1016/j.hal.2017.01.003
- Cen, J. Y., Lu, S. H., Moestrup, Ø., Jiang, T., Ho, K. C., Li, S., et al. (2024). Five *Karenia* species along the Chinese coast: With the description of a new species, *Karenia hui* sp. nov. (Kareniaceae, Dinophyta). *Harmful Algae*. 137, 102645. doi: 10.1016/j.hal.2024.102645
- Chao, A., Gotelli, N. J., Hsieh, T. C., Sander, E. L., Ma, K. H., Colwell, R. K., et al. (2014). Rarefaction and extrapolation with Hill numbers: a framework for sampling and estimation in species diversity studies. *Ecol. Monogr.* 84, 45–67. doi: 10.1890/13-0133.1
- Clément, A., Seguel, M., Arzul, G., Guzman, L., and Alarcon, C. (2000). "Widespread outbreak of a haemolytic, ichthyotoxic *Gymnodinium* sp. in southern Chile," in *Harmful algal blooms 2000*. Eds. G. M. Hallegraeff, S. I. Blackburn, C. J. Bolch and

- R. J. Lewis (Proceedings of the Ninth International Conference on Harmful Algal Blooms, Hobart, Australia), 66–69.
- Cui, Z., Xu, Q., Gibson, K., Liu, S., and Chen, N. (2021). Metabarcoding analysis of harmful algal bloom species in the Changjiang Estuary, China. *Sci. Total Environ.* 782, 146823. doi: 10.1038/nmeth.2109
- Darriba, D., Taboada, G. L., Doallo, R., and Posada, D. (2012). jModelTest 2: more models, new heuristics and high-performance computing. *Nat. Methods.* 9, 772. doi: 10.1038/nmeth.2109
- Deng, H., Guan, W., Cao, Z., Bao, M., and Chen, Q. (2016). Analysis of hydrological and meteorological factors causing *Karenia mikimotoi* bloom in 2012 along Fujian coast. *J. Mar. Sci.* 34, 28–38. doi: 10.3969/j.issn.1001-909X.2016.04.004
- Dolatabadi, F., and Attaran-Fariman, G. (2024). Bloom and phylogeny of the harmful dinoflagellate *Karenia selliformis* (Dinophyceae) isolated from Iran southeast coast (northern of Oman Sea). *Nova Hedwigia.* 119, 1–20. doi: 10.1127/nova_hedwigia/2024/0826
- Dragunow, M., Trzoss, M., Brimble, M. A., Cameron, R., Beuzenberg, V., Holland, P., et al. (2005). Investigations into the cellular actions of the shellfish toxin gymnodimine and analogues. *Environ. Toxicol. Pharmacol.* 20, 305–312. doi: 10.1016/j.etap.2005.02.008
- Feki, W., Hamza, A., Frossard, V., Abdennadher, M., Hannachi, I., Jacquot, M., et al. (2017). What are the potential drivers of blooms of the toxic dinoflagellate *Karenia selliformis*? A 10-year study in the Gulf of Gabes, Tunisia, southwestern Mediterranean Sea. *Harmful Algae.* 23, 8–18. doi: 10.1016/j.hal.2012.12.001
- Feki-Sahnoun, W., Hamza, A., Njah, H., Barra, N., Mahfoudi, M., Rebai, A., et al. (2017). A Bayesian network approach to determine environmental factors controlling *Karenia selliformis* occurrences and blooms in the Gulf of Gabès, Tunisia. *Harmful Algae.* 63, 119–132. doi: 10.1016/j.hal.2017.01.013
- Finch, S. C., Harwood, D. T., Boundy, M. J., and Selwood, A. I. (2024). A review of cyclic imines in shellfish: Worldwide occurrence, toxicity and assessment of the risk to consumers. *Mar. Drugs* 22, 129. doi: 10.3390/md22030129
- General Administration of Quality Supervision, Inspection and Quarantine of China and National Standardization Administration (2008). *National standard of the people's republic of China (GB 17378.3-2007): the specification for marine monitoring* (Beijing: The Chinese Standards Press).
- Gu, H., Wu, Y., Lü, S., Lu, D., Tang, Y. Z., and Qi, Y. (2022). Emerging harmful algal bloom species over the last four decades in China. *Harmful Algae.* 111, 102059. doi: 10.1016/j.hal.2021.102059
- Guangxi Marine Bureau (2023). *Toxic red tide monitoring information in Fangcheng sea area*. Available online at: https://hyj.gxzf.gov.cn/hykp_66917/hyhz/t16954480.shtml (Accessed February 24, 2025).
- Guillou, L., Bachar, D., Audic, S., Bass, D., Berney, C., Bittner, L., et al. (2012). The Protist Ribosomal Reference database (PR²): a catalog of unicellular eukaryote Small Sub-Unit rRNA sequences with curated taxonomy. *Nucleic Acids Res.* 41, D597–D604. doi: 10.1093/nar/gks1160
- Guillou, L., Nézan, E., Cuff, V., Erard-Le Denn, E., Cambon-Bonavita, M.-A., Gentien, P., et al. (2021). Genetic diversity and molecular detection of three toxic dinoflagellate genera (*Alexandrium*, *Dinophysis*, and *Karenia*) from French coasts. *Protist.* 153, 223–238. doi: 10.1078/1434-4610-00100
- Guindon, S., and Gascuel, O. (2003). A simple, fast, and accurate algorithm to estimate large phylogenies by maximum likelihood. *Syst. Biol.* 52, 696–704. doi: 10.1080/10635150390235520
- Guiry, M. D., and Guiry, G. M. (2025). *AlgaeBase*. Available online at: <https://www.algaebase.org> (Accessed February 24, 2025).
- Hasegawa, N., Watanabe, T., Unuma, T., Yokota, T., Izumida, D., Nakagawa, T., et al. (2022). Repeated reaching of the harmful algal bloom of *Karenia* spp. around the Pacific shoreline of Kushiro, eastern Hokkaido, Japan, during autumn 2021. *Fish Sci.* 88, 787–803. doi: 10.1007/s12562-022-01642-w
- Haywood, A. J., Steidinger, K. A., Truby, E. W., Bergquist, P. R., Bergquist, P. L., Adamson, J., et al. (2004). Comparative morphology and molecular phylogenetic analysis of three new species of the genus *Karenia* (Dinophyceae) from New Zealand. *J. Phycol.* 40, 165–179. doi: 10.1046/j.1529-8817.2004.02149.x
- He, C., Xu, S., Kang, Z. J., Song, S. Q., and Li, C. W. (2021). Prokaryotic community composition and structure during *Phaeocystis globosa* blooms in the Beibu Gulf, China. *Aquat. Microb. Ecol.* 86, 137–151. doi: 10.3354/ame01962
- Heil, C. A., Glibert, P. M., Al-Sarawi, M. A., Faraj, M., Behbehani, M., and Husain, M. (2001). First record of a fish-killing *Gymnodinium* sp. bloom in Kuwait Bay, Arabian Sea: chronology and potential causes. *Mar. Ecol. Prog. Ser.* 214, 15–23. doi: 10.3354/meps214015
- Hort, V., Abadie, E., Arnich, N., Dechraoui Bottein, M.-Y., and Amzil, Z. (2021). Chemodiversity of brevetoxins and other potentially toxic metabolites produced by *Karenia* spp. and their metabolic products in marine organisms. *Mar. Drugs* 19, 656. doi: 10.3390/md19120656
- Iwataki, M., Lum, W. M., Kuwata, K., Takahashi, K., Arima, D., Kuribayashi, T., et al. (2022). Morphological variation and phylogeny of *Karenia selliformis* (Gymnodinales, Dinophyceae) in an intensive cold-water algal bloom in eastern Hokkaido, Japan. *Harmful Algae.* 114, 102204. doi: 10.1016/j.hal.2022.102204
- Ji, Y., Che, Y. J., Wright, E. J., McCarron, P., Hess, P., and Li, A. F. (2020). Fatty acid ester metabolites of gymnodimine in shellfish collected from China and in mussels (*Mytilus galloprovincialis*) exposed to *Karenia selliformis*. *Harmful Algae.* 92, 101774. doi: 10.1016/j.hal.2020.101774
- Ji, Y., Yan, G. W., Wang, G. X., Liu, J. W., Tang, Z. X., Yan, Y. J., et al. (2022). Prevalence and distribution of domoic acid and cyclic imines in bivalve mollusks from Beibu Gulf, China. *J. Hazard. Mater.* 423, 127078. doi: 10.1016/j.jhazmat.2021.127078
- Katoh, K., and Standley, D. M. (2013). MAFFT multiple sequence alignment software version 7: improvements in performance and usability. *Mol. Biol. Evol.* 30, 772–780. doi: 10.1093/molbev/mst010
- Kezlya, E., Tseplik, N., and Kulikovskiy, M. (2023). Genetic markers for metabarcoding of freshwater microalgae: Review. *Biology.* 12, 1038. doi: 10.3390/biology12071038
- Kumar, S., Stecher, G., Li, M., Knyaz, C., and Tamura, K. (2018). MEGA X: molecular evolutionary genetics analysis across computing platforms. *Mol. Biol. Evol.* 35, 1547–1549. doi: 10.1093/molbev/msy096
- Leigh, J. W., Bryant, D., and Nakagawa, S. (2015). POPART: full-feature software for haplotype network construction. *Methods Ecol. Evol.* 6, 1110–1116. doi: 10.1111/2041-210X.12410
- Li, W. (2022). *Phytoplankton community structure and molecular diversity in Beibu Gulf. [dissertation/master's thesis]* (Gaugzhou (China: Jinan University).
- Li, S., Cen, J., Wang, J., and Lv, S. (2018). Study on acute toxicity of two *Karenia* (Dinophyceae) species to rotifer *Brachionus plicatilis*. *Mar. Environ. Science.* 37, 28–32. doi: 10.13634/j.cnki.mes20180105
- Li, J., Lai, J. X., Xu, G. L., Xu, M. B., Wu, M., Yan, X. M., et al. (2024). Detecting the *Phaeocystis globosa* bloom and characterizing its bloom condition in the northern Beibu Gulf using MODIS measurements. *Mar. Pollut. Bull.* 209, 117273. doi: 10.1016/j.marpolbul.2024.117273
- Li, X., Yan, T., Lin, J., Yu, R., and Zhou, M. (2017). Detrimental impacts of the dinoflagellate *Karenia mikimotoi* in Fujian coastal waters on typical marine organisms. *Harmful Algae.* 61, 1–12. doi: 10.1016/j.hal.2016.11.011
- Li, X. D., Yan, T., Yu, R. C., and Zhou, M. J. (2019). A review of *karenia mikimotoi*: Bloom events, physiology, toxicity and toxic mechanism. *Harmful Algae.* 90, 101702. doi: 10.1016/j.hal.2019.101702
- Li, Y., Zhu, S., Hang, X., Sun, L., Li, X., Luo, X., et al. (2023). Variation of local wind fields under the background of climate change and its impact on algal blooms in Lake Taihu, China. *Water.* 15, 4258. doi: 10.3390/w15244258
- Lin, S. (2024). A decade of dinoflagellate genomics illuminating an enigmatic eukaryote cell. *BMC Genomics* 25, 932. doi: 10.1186/s12864-024-10847-5
- Lin, Y., Cen, J., Wang, J., Liang, Q., and Lv, S. (2020). Preliminary study on interspecific relationship and hemolytic activity of four *Karenia* species from South China Sea. *Oceanologia Et Limnologia Sinica.* 51, 1402–1411. doi: 10.11693/hyhz20200100002
- Ling, C., and Trick, C. G. (2010). Expression and standardized measurement of hemolytic activity in *Heterosigma akashiwo*. *Harmful Algae.* 9, 522–529. doi: 10.1016/j.hal.2010.04.004
- Liu, Q. Y., Chen, Z. M., Li, D. W., Li, A. F., Ji, Y., Li, H. Y., et al. (2023). Toxicity and potential underlying mechanism of *Karenia selliformis* to the fish *Oryzias melastigma*. *Aquat. Toxicol.* 262, 106643. doi: 10.1016/j.aquatox.2023.106643
- Liu, Y., Hu, Z., Deng, Y., and Tang, Y. Z. (2020). Evidence for resting cyst production in the cosmopolitan toxic dinoflagellate *Karolodinium veneficum* and the cyst distribution in the China seas. *Harmful Algae.* 93, 101788. doi: 10.1016/j.hal.2020.101788
- Lü, S., Cen, J., Wang, J., and Ou, L. (2019). The research status quo, hazard, and ecological mechanisms of *Karenia mikimotoi* red tide in coastal waters of China. *Oceanologia Et Limnologia Sinica.* 50, 487–494. doi: 10.11693/hyhz20181000255
- MacKenzie, L., Haywood, A., Adamson, J., Truman, P., Till, D., Satake, M., et al. (1996). "Gymnodimine contamination of shellfish in New Zealand," in *Harmful and toxic algal blooms proceeding of the seventh international conference on toxic phytoplankton*. Eds. T. Yasumoto, Y. Oshima and Y. Fukuyo (Intergovernmental Oceanographic Commission of UNESCO, Sendai, Japan), 97–100.
- Mardones, J. I., Norambuena, L., Paredes, J., Fuenzalida, G., Dorantes-Aranda, J. J., Chang, K. J. L., et al. (2020). Unraveling the *Karenia selliformis* complex with the description of a non-gymnodimine producing Patagonian phylogroup. *Harmful Algae.* 98, 101892. doi: 10.1016/j.hal.2020.101892
- Martin, M. (2011). Cutadapt removes adapter sequences from high-throughput sequencing reads. *EMBnet J.* 17, 10–12. doi: 10.14806/ej.17.1.200
- Medhioub, A., Medhioub, W., Amzil, Z., Sibat, M., Bardouil, M., Ben Neila, I., et al. (2009). Influence of environmental parameters on *Karenia selliformis* toxin content in culture. *Cah. Biol. Mar.* 50, 333–342.
- Miles, C. O., Wilkins, A. L., Stirling, D. J., and MacKenzie, A. L. (2000). New analogue of gymnodimine from a *Gymnodinium* species. *J. Agric. Food Chem.* 48, 1373–1376. doi: 10.1021/jf991031k
- Miles, C. O., Wilkins, A. L., Stirling, D. J., and MacKenzie, A. L. (2003). Gymnodimine C, an isomer of Gymnodimine B, from *Karenia selliformis*. *J. Agric. Food Chem.* 51, 4838–4840. doi: 10.1021/jf030101r
- Molgó, J., Marchot, P., Araújo, R., Benoit, E., Iorga, B. I., Zakarian, A., et al. (2017). Cyclic imine toxins from dinoflagellates: a growing family of potent antagonists of the nicotinic acetylcholine receptors. *J. Neurochem.* 142, 41–51. doi: 10.1111/jnc.13995

- National Environmental Protection Agency (2004). *GB 3097-1997, Marine water quality standard* (Beijing: China Environmental Press).
- Natsuike, M., Kanamori, M., Akino, H., Sakamoto, S., and Iwataki, M. (2023). Lethal effects of the harmful dinoflagellate *Karenia selliformis* (Gymnodiniales, Dinophyceae) on two juvenile kelp sporophytes *Saccharina japonica* and *S. sculpera* (Laminariales, Phaeophyceae). *Reg. Stud. Mar. Sci.* 65, 103094. doi: 10.1016/j.rsm.2023.103094
- Niu, Z., Guan, W. B., Wang, J. X., Yuan, Y. Q., Kong, F. Z., Liu, C., et al. (2022). Dynamics of *Phaeocystis globosa* bloom and implications for its seed sources in the Beibu Gulf, China. *J. Oceanol. Limnol.* 40, 2385–2400. doi: 10.1007/s00343-022-1447-0
- Nunn, G., Theisen, B., Christensen, B., and Arctander, P. (1996). Simplicity-correlated size growth of the nuclear 28S ribosomal RNA D3 expansion segment in the crustacean order Isopoda. *J. Mol. Evol.* 42, 211–223. doi: 10.1007/BF02198847
- Ohnishi, T., Taniuchi, Y., Watanabe, T., Shikata, T., and Kasai, H. (2024). Experimental assessment of copepod survival in response to the harmful dinoflagellate *Karenia selliformis* from the southeastern coast of Hokkaido, Japan. *Plankton Benthos Res.* 19, 88–97. doi: 10.3800/pbr.19.88
- Ok, J. H., Jeong, H. J., Lim, A. S., Kang, H. C., You, J. H., Park, S. A., et al. (2023). Lack of mixotrophy in three *Karenia* species and the prey spectrum of *Karenia mikimotoi* (Gymnodiniales, Dinophyceae). *Algae*. 38, 39–55. doi: 10.4490/algae.2023.38.2.28
- Ok, J. H., Jeong, H. J., You, J. H., Park, S. A., Kang, H. C., Eom, S. H., et al. (2024). Interactions between the calanoid copepod *Acartia hongii* and the bloom-forming dinoflagellates *Karenia bicuneiformis* and *K. selliformis*. *Mar. Biol.* 171, 112. doi: 10.1007/s00227-024-04427-0
- Orlova, T. Y., Aleksanin, A. I., Lepskaya, E. V., Efimova, K. V., Selina, M. S., Morozova, T. V., et al. (2022). A massive bloom of *Karenia* species (Dinophyceae) off the Kamchatka coast, Russia, in the fall of 2020. *Harmful Algae*. 120, 102337. doi: 10.1016/j.hal.2022.102337
- Park, S. A., Ok, J. H., Eom, S. H., Kwon, M. J., You, J. H., Kang, H. C., et al. (2024). Differential interactions between the bloom-forming dinoflagellates *Karenia bicuneiformis* and *Karenia selliformis* and heterotrophic dinoflagellates. *Algae*. 39, 255–275. doi: 10.4490/algae.2024.39.11.30
- Posit team (2024). *RStudio: Integrated development environment for R* (Boston, MA: Posit Software, PBC). Available at: <http://www.posit.co/> (Accessed April 18, 2025).
- R Core Team (2024). *R: A language and environment for statistical computing* (Vienna, Austria: R Foundation for Statistical Computing). Available at: <https://www.R-project.org/> (Accessed April 18, 2025).
- Ren, X., Yu, Z., Song, X., Zhu, J., Wang, W., and Cao, X. (2022). Effects of modified clay on the formation of *Phaeocystis globosa* colony revealed by physiological and transcriptomic analyses. *Sci. Total Environ.* 838, 155985. doi: 10.1016/j.scitotenv.2022.155985
- Rolton, A., Rhodes, L., Hutson, K. S., Biessy, L., Bui, T., MacKenzie, L., et al. (2022). Effects of harmful algal blooms on fish and shellfish species: A case study of New Zealand in a changing environment. *Toxins*. 14, 341. doi: 10.3390/toxins14050341
- Ronquist, F., Teslenko, M., van der Mark, P., Ayres, D. L., Darling, A., Höhna, S., et al. (2012). MrBayes 3.2: Efficient Bayesian phylogenetic inference and model choice across a large model space. *Syst. Biol.* 61, 539–542. doi: 10.1093/sysbio/sys029
- Sakamoto, S., Lim, W. A., Lu, D., Dai, X., Orlova, T., and Iwataki, M. (2021). Harmful algal blooms and associated fisheries damage in East Asia: Current status and trends in China, Japan, Korea and Russia. *Harmful Algae*. 102, 101787. doi: 10.1016/j.hal.2020.101787
- Scholich, C. A., Herzog, M., Sogin, M., and Anderson, D. M. (1994). Identification of group- and strain-specific genetic markers for globally distributed *Alexandrium* (Dinophyceae). II. sequence analysis of a fragment of the LSU rRNA gene. *J. Phycology*. 30, 999–1011. doi: 10.1111/j.0022-3646.1994.00999.x
- Seki, T., Satake, M., Mackenzie, L., Kaspar, H. F., and Yasumoto, T. (1995). Gymnodimine, a new marine toxin of unprecedented structure isolated from New Zealand oysters and the dinoflagellate. *Gymnodinium Tetrahedron Lett.* sp. 36. doi: 10.1016/0040-4039(95)01434-J
- Smith, K. F., Stuart, J., and Rhodes, L. L. (2024). Molecular approaches and challenges for monitoring marine harmful algal blooms in a changing world. *Front. Protistol.* 1. doi: 10.3389/frprot.2023.1305634
- Song, X., Xu, Z., Zhang, W., and Tong, M. (2023). Regulation of photosynthetic and hemolytic activity of *Phaeocystis globosa* under different light spectra. *New Phytol.* 239, 1852–1868. doi: 10.1111/nph.19056
- Stamatakis, A. (2014). RAXML version 8: a tool for phylogenetic analysis and post-analysis of large phylogenies. *Bioinformatics*. 30, 1312–1313. doi: 10.1093/bioinformatics/btu033
- Stern, R. F., Horak, A., Andrew, R. L., Coffroth, M. A., Andersen, R. A., Küpper, F. C., et al. (2010). Environmental barcoding reveals massive dinoflagellate diversity in marine environments. *PLoS One* 5, e13991. doi: 10.1371/journal.pone.0013991
- Stoeck, T., Bass, D., Nebel, M., Christen, R., Jones, M. D., Breiner, H. W., et al. (2010). Multiple marker parallel tag environmental DNA sequencing reveals a highly complex eukaryotic community in marine anoxic water. *Mol. Ecol.* 19, 21–31. doi: 10.1111/j.1365-294X.2009.04480.x
- Stumpf, R. P., Li, Y., Kirkpatrick, B., Litaker, R. W., Hubbard, K. A., Currier, R. D., et al. (2022). Quantifying *Karenia brevis* bloom severity and respiratory irritation impact along the shoreline of Southwest Florida. *PLoS One* 17, e0260755. doi: 10.1371/journal.pone.0260755
- Su, Q., Lei, X., Liu, G., Sun, Y., Lao, Q., and Sun, T. (2022). Characteristics of red tide disaster in coastal waters of Beibu Gulf of Guangxi in recent 20 years. *Guangxi Sci.* 29, 552–557. doi: 10.13656/j.cnki.gxkx.20220720.018
- Takagi, S., Kuroda, H., Hasegawa, N., Watanabe, T., Unuma, T., Taniuchi, Y., et al. (2022). Controlling factors of large-scale harmful algal blooms with *Karenia selliformis* after record-breaking marine heatwaves. *Front. Mar. Sci.* 9. doi: 10.3389/fmars.2022.939393
- Tang, Y. Z., Gu, H., Wang, Z., Liu, D., Wang, Y., Lu, D., et al. (2021a). Exploration of resting cysts (stages) and their relevance for possibly HABs-causing species in China. *Harmful Algae*. 107, 102050. doi: 10.1016/j.hal.2021.102050
- Tang, Z. X., Qiu, J. B., Wang, G. X., Ji, Y., Hess, P., and Li, A. F. (2021b). Development of an efficient extraction method for harvesting Gymnodimine-A from large-scale cultures of *Karenia selliformis*. *Toxins*. 13, 793. doi: 10.3390/toxins13110793
- Tatters, A. O., Muhlstein, H. I., and Tomas, C. R. (2010). The hemolytic activity of *Karenia selliformis* and two clones of *Karenia brevis* throughout a growth cycle. *J. Appl. Phycol.* 22, 435–442. doi: 10.1007/s10811-009-9476-z
- Uribe, J. C., and Ruiz, M. (2001). *Gymnodinium* brown tide in the Magellanic fjords, southern Chile. *Rev. Biol. Mar. Oceanogr.* 36, 155–164. doi: 10.4067/S0718-19572001000200004
- Vellojin, J. P., Mardones, J. I., Vargas, V., Leal, P. P., Corredor-Acosta, A., and Iriarte, J. L. (2023). Potential effects of climate change on the growth response of the toxic dinoflagellate *Karenia selliformis* from Patagonian waters of Chile. *Prog. Oceanogr.* 211, 102956. doi: 10.1016/j.pocan.2022.102956
- Wolny, J. L., Scott, P. S., Tustison, J., and Brooks, C. R. (2015). Monitoring the 2007 Florida east coast *Karenia brevis* (Dinophyceae) red tide and neurotoxic shellfish poisoning (NSP) event. *Algae*. 30, 49–58. doi: 10.4490/algae.2015.30.1.049
- Wu, X. Z., Wang, G. X., Qiu, J. B., Li, A. F., and Hess, P. (2024). Effects of culture systems and nutrients on the growth and toxin production of *Karenia selliformis*. *Toxins*. 16, 518. doi: 10.3390/toxins16120518
- Xu, Y., Dzhenbekova, N., Smith, K. F., Gu, H., John, U., Xie, H., et al. (2024). Biodiversity and hemolytic toxicity of the genus *Heterocapsa* (Dinophyceae) in the Beibu Gulf, China. *Mar. Drugs* 22, 514. doi: 10.3390/md22110514
- Xu, Y., He, X., Lee, W. H., Chan, L. L., Lu, D., Wang, P., et al. (2021a). Ciguatera-producing dinoflagellate *Gambierdiscus* in the Beibu Gulf: First report of toxic *Gambierdiscus* in Chinese waters. *Toxins*. 13, 643. doi: 10.3390/toxins13090643
- Xu, Y., Wei, G., Wang, Y., Jia, Y., Gao, H., Zhang, T., et al. (2021b). Pollution of lipophilic shellfish toxins in Qinzhou Bay: Seawater and *Crassostrea hongkongensis*. *Oceanologia Et Limnologia Sinica*. 52, 144–152. doi: 10.11693/hyhz20200400126
- Xu, Y., Zhang, T., and Zhou, J. (2019). Historical occurrence of algal blooms in the northern Beibu Gulf of China and implications for future trends. *Front. Microbiol.* 10. doi: 10.3389/fmicb.2019.00451
- Yu, Z., Tang, Y., and Gobler, C. J. (2023). Harmful algal blooms in China: History, recent expansion, current status, and future prospects. *Harmful Algae*. 129, 102499. doi: 10.1016/j.hal.2023.102499
- Zhang, Q., Liu, C., Qiu, L., Zhang, W., Sun, L., Gu, H., et al. (2025). Genetic diversity and distribution of *Karenia* in the eastern coastal seas of China and implications for the trends in *Karenia* blooms under global environmental changes. *J. Environ. Manage.* 373, 123465. doi: 10.1016/j.jenvman.2024.123465
- Zhang, W., Zhang, Q., Smith, K. F., Qiu, L., Liu, C., Yin, X., et al. (2022). Development of specific DNA barcodes for the Dinophyceae family Kareniaceae and their application in the South China Sea. *Front. Mar. Sci.* 9. doi: 10.3389/fmars.2022.851605